Available online at www.sciencedirect.com

ScienceDirect

Catalysis Today 128 (2007) 216–222

CATALYSIS TODAY

www.elsevier.com/locate/cattod

Partial oxidation of methane towards hydrogen production over a promising class of catalysts: Rh supported on Ti-modified MgO

C. Mateos-Pedrero *, C. Cellier, P. Eloy, P. Ruiz

Unité de catalyse et chimie des matériaux divisés, Université catholique de Louvain,
Croix du Sud 2/17, B-1348 Louvain-la-Neuve, Belgium

Abstract

The partial oxidation of methane over the supported Rh (0.8 wt.%) catalysts was investigated. Two kinds of supports were used, MgO and Ti-modified MgO (prepared by grafting technique). Among the Ti-modified MgO supports, two different compounds were used as source of Ti: inorganic (chloride) and organic (alkoxide). The catalytic performance of Rh-supported catalysts depends on the support and varies in the sequence: Ti-MgO/I > Ti-MgO/O > MgO. Ti-containing catalysts exhibited higher activity and selectivity compared to MgO, which is especially noticeable at low temperature. Possible explanations for the phenomena observed were proposed on the basis of characterization results.

Keywords: Partial methane oxidation; Ti-modified MgO supports; Rh-supported catalysts; Activity; Selectivity

---

1. Introduction

The partial oxidation of methane (POM) constitutes a proper way to produce synthesis gas. This reaction is mildly exothermic and provides a suitable H_2/CO ratio for the methanol and Fischer–Tropsch syntheses. These characteristics make POM an attractive and feasible alternative to steam reforming reaction in order to produce syngas. Rh-supported catalysts are commonly used in POM. It is accepted that the activity of these catalysts depends on the nature of the support. The effect of support on the partial oxidation of methane to syngas over Rh-supported catalysts was investigated in [1]; it was found that the reducible oxides supported rhodium catalysts provided, in general, much lower activities and selectivities (to H_2 and CO) than those supported on irreducible oxides. In the POM reaction, the sintering, the loss and changes in oxidation state of the metal active phase are common factors leading to the deactivation of the catalyst. The most obvious way to lessen these phenomena is to work at low temperatures, however the methane partial oxidation reaction has to proceed at high temperatures (usually higher than 700 °C) to get a meaningful conversion of methane [1]. The 1% Rh/MgO has been previously identified as an active and selective catalyst for POM reaction, although in that case very high temperatures are required [2]. We report results will show that the activity and the selectivity of Rh-based catalysts can be improved (particularly at low temperatures), by using Ti-modified MgO as supports. Ti-modified MgO samples were prepared by grafting MgO with Ti from two different precursors: Ti-chloride (inorganic) and Ti-isopropoxide (organic) before impregnating rhodium. The resulting Rh/Ti-MgO catalysts provide higher activities and selectivities towards H_2 and CO than Rh/MgO.

2. Experimental

2.1. Catalyst preparation

The Ti-modified MgO samples were prepared following the grafting technique. For the synthesis of such compounds two different Ti-precursors were used: $TiCl_4$ (inorganic method, I), or $Ti[OCH(CH_3)_2]_4$ (organic method, O). Both Ti-modified samples contain the same titanium amount (8.5 wt.% of TiO_2),

---

* Corresponding author. Tel.: +32 10473658.
E-mail address: mateos@cata.ucl.ac.be (C. Mateos-Pedrero).

0920-5861/$ – see front matter
doi:10.1016/j.cattod.2007.06.066

which was calculated in a similar way as described in [3]. The preparation procedure of these samples was as follows.

2.1.1. Inorganic method

The inorganically modified support was prepared by grafting of an MgO support from UCB with $TiCl_4$ (Across Organics, 99+%). Four grams of the support were dipped into a solution containing the adequate amount of $TiCl_4$ in *n*-hexane (Merck, pure grade). After 3 h of stirring at rt, the solvent was gently removed under reduced pressure in a rotavapor at 50 °C. The resulting solid was dried at 110 °C for 16 h and finally calcined at 500 °C for 20 h. The sample is denoted as Ti-MgO/I.

2.1.2. Organic method

The same MgO support was used. The organically modified support was prepared starting from $Ti[OCH(CH_3)_2]_4$ (Aldrich, 99+%) in isopropanol (Aldrich, 99+%), following an analogous procedure as described above, but in this case the solvent was evaporated at 70 °C. The sample is denoted as Ti-MgO/O.

2.1.3. Preparation of Rh-supported catalysts

3.8 g of the support (Ti-MgO/I, Ti-MgO/O and bare MgO) were dipped into 400 cm^3 of deionized water and the adequate amount of $(NH_4)3RhCl_6{\cdot}3H_2O$ (Across, 28 wt.% of Rh) was added in order to obtain theoretically 0.8 wt.% of Rh catalysts. After stirring at rt for 2 h, the solvent was evaporated in a rotavapor at 35 °C. The recovered solid was dried at 110 °C for 16 h before its calcination in air at 700 °C during 4 h. Samples are denoted as Rh/MgO, Rh/Ti-MgO/I and Rh/Ti-MgO/O. Since the Rh loading in the catalysts is too low for XRD analysis, one catalyst containing 10 wt.% of Rh on MgO was prepared following the same procedure as described above. This catalyst is labeled as Rh(10)/MgO.

2.2. Catalysts characterization

XRD, BET, TPR, H_2 chemisorption and XPS were used. The characterization methods are described in detail in [3]. The average noble metal particle diameter was estimated from the XPS measurements using the method presented in [4].

2.3. Catalytic activity

The gaseous feed was composed of a mixture of 5 vol.% of CH_4 (Indugas, 99.5%) and 2.5 vol.% of O_2 (Indugas, 99.5%) diluted in nitrogen (Indugas, 99.9%) for a total flow of 100 ml/min. The amount of the catalyst was 100 mg (particle size between 200 and 215 μm). Before starting the reaction catalysts were reduced by contacting them with a pure H_2 flow (Indugas, 99.5%) for 3 h at 600 °C (slope 10°/min). The catalytic activity was measured between 400 and 700 °C, and then the reactor was cooled down under the reaction conditions. Reproducibility was checked using identical conditions and catalysts from the same batch, and results showing the measured performances accurate within ranges of about 1% (in relative) for both CH_4 and O_2 conversions and within ranges of about 3% (in relative) for the yields in H_2 and CO. The range of accuracy on the selectivities was thus about 8% (in relative).

3. Results

3.1. Characterization results for Ti-MgO samples: Ti-MgO/I and Ti-MgO/O

The textural properties of the samples are summarized in Table 1. All solids present type II isotherms, associated to mesoporous solids, according to IUPAC classification [5]. Hysteresis loops are H_3 type, characteristic of slit shaped, non-uniform pores [5]. The textural properties of Ti-MgO samples depend on the Ti-precursor. The inorganically modified MgO (Ti-MgO/I) has similar textural properties to the bare MgO (Table 1). On the contrary, the surface area for the organically modified MgO (Ti-MgO/O) is lower than that of the bare MgO; parallel to the decrease in the surface area, there is a shortening of the pore volume and a broadening of the pore size. Moreover, for bare MgO, the pore size distribution was monomodal, but that of the Ti-MgO oxides was bimodal.

The X-ray diffraction patterns for calcined MgO exhibit the main peaks for periclase ($2\theta = 43.1°$ and 62.3°, respectively). Regarding Ti-MgO samples, together with the characteristic peaks of periclase, we can observe the presence of very broad peaks, which are characteristic of mixed phases Mg-Ti-O. The presence of $MgTi_2O_3$ (geikielite) is observed in both samples. Moreover, the XRD patterns for Ti-MgO/O show the appearance of $MgTi_2O_5$ karooite ($2\theta = 25.4°$, 32.6°, 48.6° and 59.7°, respectively) and those of Ti-MgO/I revealed the appearance of Mg_2TiO_4 qandilite ($2\theta = 35.2°$ and 18.2°, respectively).

A study of the surface composition of Ti-MgO samples was made by XPS and the results are presented in Table 1; data corresponding to pure MgO are also shown as reference.

Table 1
Physico-chemical properties for MgO-based samples

Sample	S_{BET} (m^2/g)	D_p (Å)	V_p (cm^3/g)	Ti/Mg (at. ratio)	BE Mg2p (eV)	BE Ti2$p_{3/2}$ (eV)	XRD (detected phases)
MgO	56	248	0.36	–	88.0	–	MgO[a]
Ti-MgO/I	54	245	0.34	0.22	88.3	458.2	MgO[a] $MgTiO_3$[b] Mg_2TiO_4[c]
Ti-MgO/O	45	224	0.25	0.08	88.2	458.1	MgO[a] $MgTiO_3$[b] $MgTi_2O_5$[d]

[a] Periclase.
[b] Geikielite.
[c] Qandilite.
[d] Karooite.

Table 2
Physico-chemical properties for Rh-supported catalysts

Catalyst	S_{BET} (m^2/g)	D_p (Å)	V_p (cm^3/g)	Dispersion (%)	TPR (°C)	XRD (detected phases)
Rh/MgO	44	310	0.39	17	380	MgO
Rh/Ti-MgO/I	52	249	0.34	18	414	MgO $MgTiO_3$ Mg_2TiO_4
Rh/Ti-MgO/O	39	294	0.19	17	388	MgO $MgTiO_3$ $MgTi_2O_5$

XPS Ti/Mg atomic ratio is greatly higher in Ti-MgO/I than in Ti-MgO/O, reflecting that the surface composition of Ti-MgO samples depends on the Ti-precursor. The inorganic precursor (Ti-MgO/I) gives rise to a richer Ti surface compared with that of Ti-MgO/O (Table 1). Regarding binding energies, there are three different oxygen signals at about 529.6, 531.4 and 532.4 eV. Binding energy for O1s at 529.6 and at 531.4 eV agrees with the O1s assigned to TiO_2 and MgO, respectively. The band at about 532 eV is attributed to carbonates in [6]. Since, in our samples, the presence of carbon as carbonate is confirmed by the existence of a C1s signal at about 290.1 eV, our O1s signal at 532.4 eV could be due to these species. Values obtained for $Ti2p_{3/2}$ binding energy suggest that oxidation state for such a species is +4 [7,8]. The binding energy values obtained for $Ti2p_{3/2}$ and O1s (529.6 eV) strongly suggest the existence of TiO_2 on the surface of our samples. Since no TiO_2 crystallites are observed by XRD, the titania particles present in our samples should be very small (<5 nm). The binding energy for Mg_2s (88.2 eV) is similar for both Ti-containing samples and corresponds with that usually assigned to MgO.

3.2. Characterization results for Rh-supported catalysts

The textural properties of Rh-supported samples are summarized in Table 2. The specific surface area for Rh/MgO and Rh/Ti-MgO/O samples diminished after impregnating rhodium; this loss in the specific surface area was accompanied by the broadening in the pore size. The textural properties of the Rh/Ti-MgO/I sample were not substantially altered by the impregnation of Rh.

The detected phases in the XRD patterns of the Rh-supported catalysts are listed in Table 2. As already mentioned, since in our catalysts the Rh loading is very low, a Rh(10)/MgO sample (10 wt.% of Rh) was prepared in order to check if the formation of $MgRh_2O_4$ occurs under the present conditions. The XRD patterns of Rh(10)/MgO show the main peaks of Rh_2O_3 at $2\theta = 35°$ (1 1 0) and 33° (1 0 4) together with those of the support (MgO), but no peaks belonging to $MgRh_2O_4$ were detected. The calcination of this sample at 800 °C resulted in the appearance of broad peaks at $2\theta = 34°$, 42.4° and 18°, being characteristic of $MgRh_2O_4$. XRD patterns for fresh, reduced and tested Rh/Ti-MgO/I and Rh/Ti-MgO/O samples show the same phases as those described for supports.

Rh dispersions determined through H_2 chemisorption analyses are presented in Table 2. The dispersion of Rh is almost the same in all catalysts (17%); it means that the number of metal sites exposed after reduction over Rh on different supports is quite similar.

The TPR hydrogen profile for these catalysts revealed a single peak of reduction (Fig. 1). It is found that reduction of Rh on MgO occurs at about 380 °C. Addition of Ti to the MgO led to a shift of the reduction peak of Rh towards somewhat higher temperature (414 °C) in Rh/Ti-MgO/). On the contrary, in the case of Rh/Ti-MgO/O, no notable changes are observed and Rh is reduced at the same temperature range as over MgO (about 388 °C). These results show that the effect of adding Ti to the MgO on the reducibility of Rh depends on the Ti-precursor. In Figs. 2–4 the spectra from the binding energy (BE) region of the Rh3d peak are shown for fresh (samples after calcination in air for 4 h at 700 °C), reduced (samples after H_2-reduction for 3 h at 600 °C), and tested (samples recovered after POM reaction) samples. $Rh3d_{5/2}$ BE values for metallic Rh are 307.0–307.3 eV [9] and for Rh_2O_3 they are 308.6–309.4 eV [9,10]. The existence of a reduction-resistive oxide phase (identified as RhO_2) has been reported in [9,11]. $Rh3d_{5/2}$ BE in this irreducible phase is 309.3–309.9 eV [9,11]. On the fresh samples the Rh3d transition is intensive and the maximum of the $Rh3d_{5/2}$ component appears to be centered at 309.4 eV. This value of BE could be attributed, in principle, at Rh_2O_3 (reducible Rh) and/or RhO_2 (irreducible Rh). However, Rh on these samples is mainly reducible as indicated by the shift of the $Rh3d_{5/2}$ from its initial BE of 309.6 eV to lower values (306.5 eV) in the H_2-reduction. This strongly

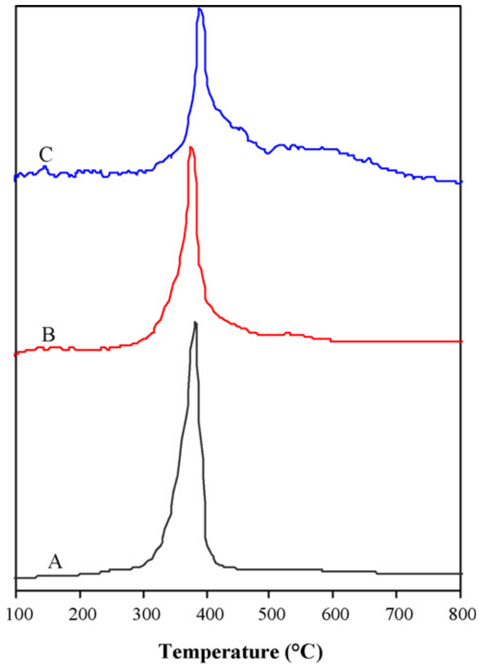

Fig. 1. TPR-H_2 profiles for Rh/MgO (A), Rh/10Ti-MgO/O (B) and Rh/10Ti-MgO/I (C).

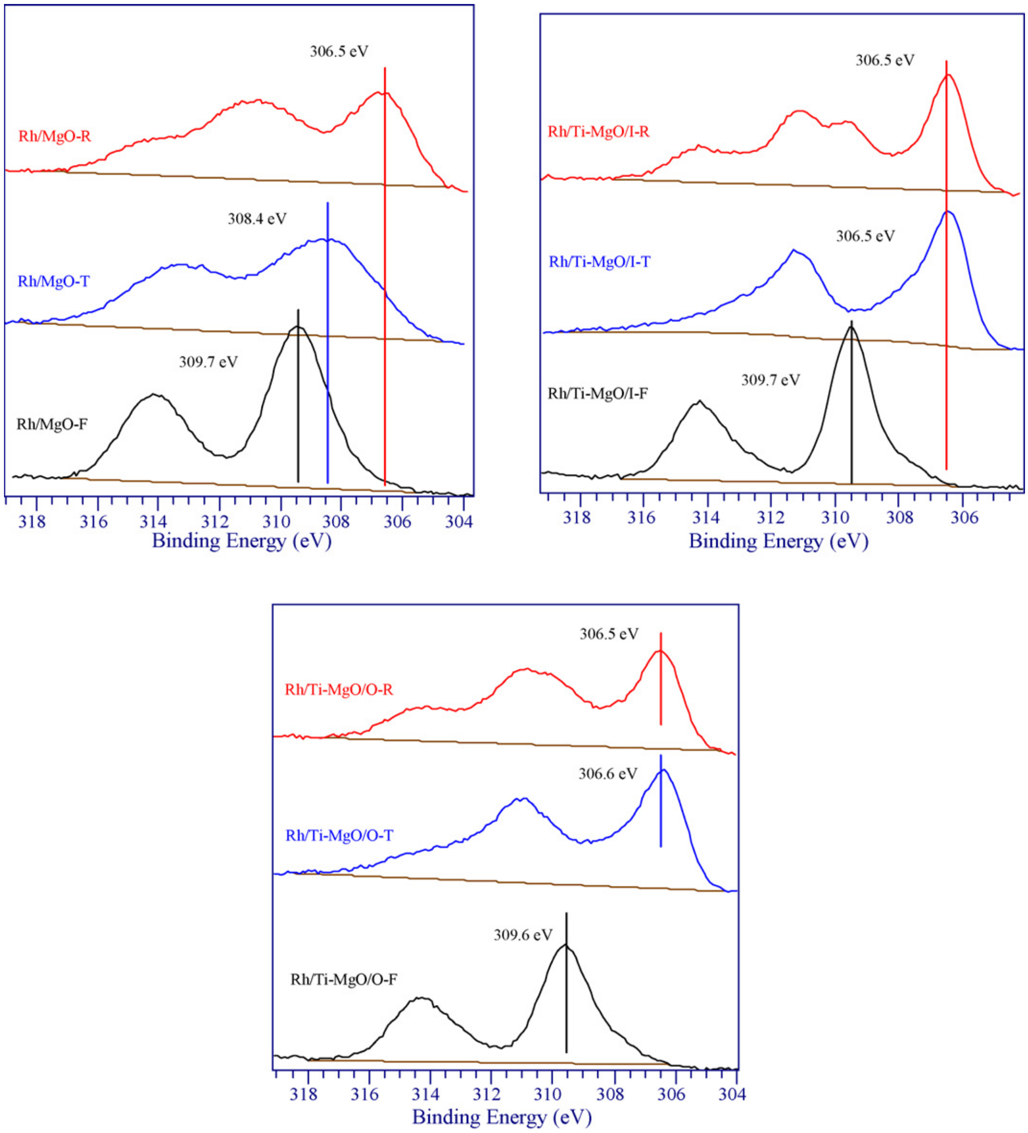

Figs. 2–4. Rh3d core level for Rh-supported catalysts: fresh (F), reduced (R) and after test (T).

suggests that the $Rh3d_{5/2}$ BE of 309.6 eV corresponds mainly to Rh_2O_3 (reducible). The spectrum of the fresh Rh/Ti-MgO samples consists of a doublet with an $Rh3d_{5/2}$ BE of 309.6 eV, while it also contains a very small signal (5% of the total area) with a BE of 307.7 eV (Figs. 2–4, Table 3). The higher value corresponds with Rh_2O_3, as mentioned above, and the lower is between the values of metallic Rh and Rh_2O_3 (probably Rh^+).

After the H_2-reduction of the fresh samples the lower BE component of the Rh3d peak shifts to 306.5 eV, which is notably lower than that commonly attributed to metallic rhodium. The shape of the spectra corresponding to the reduced samples (Figs. 2–4) reveals that Rh appears in several chemical states. Give as an example the spectrum for Rh/Ti-MgO/I, which can clearly be resolved and the peak positions can be obtained by fitting. In the fitting procedure the relative area, as well as the distance between the $Rh3d_{5/2}$ and the $Rh3d_{3/2}$ components were constrained virtually to the same values as for the fresh samples. In the fitted spectra corresponding to the Rh/Ti-MgO/I sample (not shown here) the following components of $Rh3d_{5/2}$ peak can be distinguished. The higher component (at 309.6 eV) coincides with the peak position of Rh_2O_3. The intermediate component (at 307.7 eV) is between the values of metallic Rh and Rh_2O_3. Finally, the component at 306.5 eV has a BE considerably lower than the usual value of metallic Rh. The Rh_3d peak for the other samples is somewhat more complex and hence its decomposition did not result so evident. However, the broadness of the lines suggests the presence of Rh in other oxidation states along with reduced Rh, as already mentioned for Rh/Ti-MgO/I.

The spectra for the catalysts after test reveal the different behaviour of Rh when supported on Ti-modified MgO or on pure MgO. For the Rh/MgO catalyst the Rh3d peak is clearly shifted towards higher BE values (308.4 eV), revealing that a large part of Rh has been reoxidized during reaction. However, it is noteworthy that, when Rh is supported on Ti-modified MgO the most part of it remains reduced, as evidenced by the maximum of the peak is still centered at 306.5 eV.

Table 3
Summary of XPS data for Rh-supported catalysts

Sample	Ti/Mg (at. ratio)	Rh/Mg (at. ratio)	BE Mg2p (eV)	BE Ti2p$_{3/2}$ (eV)	BE Rh3p$_{5/2}$ (eV)	D_{Rh}^{*} (nm)
Rh/MgO-F	–	0.013	88.0	–	309.6	10
Rh/MgO-R	–	0.013	88.2	–	306.5	11
Rh/MgO-T	–	0.014	88.2	–	308.4	10
Rh/Ti-MgO/I-F	0.21	0.014	88.3	458.2	309.6	9
Rh/Ti-MgO/I-R	0.21	0.013	88.5	458.5	306.5	10
Rh/Ti-MgO/I-T	0.22	0.013	88.4	458.4	306.5 (53%)[a] (63%)[b]	8
Rh/Ti-MgO/O-F	0.09	0.011	88.3	458.1	309.5	12
Rh/Ti-MgO/O-R	0.09	0.012	88.4	458.3	306.5	10
Rh/Ti-MgO/O-T	0.09	0.013	88.4	458.2	306.6(31%)[a] (57%)[b]	11

Mg + Ti, for Rh supported on MgO or Ti/MgO, respectively; *average of Rh particle diameter estimated from the XPS measurements using the method described in [4]. F, R and T stand for fresh, reduced and tested catalysts, respectively. Values in parentheses represent the percentage of metallic Rh found in the catalyst recovered after test at 550 °C (a) or 700 °C (b).

Table 3 reports the surface atom percentage composition of the catalysts: fresh, reduced and after test. The impregnation of Rh on the supports does not significantly change atomic percentage surface compositions, with the exception indicated hereafter. The Ti/Mg atomic ratio in the Rh/Ti-MgO/O sample shows a surface enrichment of Ti after impregnating rhodium. The C and Rh atomic percentage surface composition remains unchanged regardless of the catalysts are submitted to reduction or test.

3.3. Catalytic performance of Rh-supported catalysts

The results obtained over Rh-supported catalysts in the POM reaction are presented in Figs. 5 and 6. The inorganic catalyst (Rh/Ti-MgO/I), exhibited higher conversions than those of the organic one (Rh/Ti-MgO/O), particularly at 550 °C (Fig. 5). Rh/MgO catalyst is not active in POM at temperatures lower than 600 °C. However, increasing the temperature up to 600 °C sharply activates this catalyst and at this temperature its activity is only a little lower compared to that of Rh/Ti-MgO/O. The CH_4 conversion increases continuously with the temperature for all catalysts, but the Ti-modified catalysts are still more active. Concerning the yield and the selectivity towards H_2 and CO, the same trends were observed for both Ti-modified catalysts. A higher amount of H_2 and CO is produced when the temperature increases. Nonetheless the Rh/Ti-MgO/I catalyst is significantly more selective towards H_2 and CO than Rh/Ti-MgO/O, particularly at very low temperature (Fig. 5). It is noteworthy that Rh/MgO does not produce H_2 or CO at temperatures lower than 600 °C (only CO_2 and H_2O are produced on this catalyst), which indicates that a higher temperature is required for activating this catalyst. At temperatures higher than 600 °C (Fig. 6), Rh/MgO exhibits a selectivity towards H_2 and CO comparable to that of the Rh/Ti-MgO/O catalyst, but the Rh/Ti-MgO/I catalyst is still more selective.

4. Discussion

4.1. Effect of the presence of Ti on the solid state properties of supports

The modification of the textural properties of Ti-MgO samples as a consequence of adding titanium to MgO depends on the Ti-precursor (Table 1). The textural properties of the Ti-MgO/I (inorganic Ti-precursor) are very similar to those of bare MgO, but the addition of Ti to MgO caused a substantial decrease in the surface area and in the porosity when the organic Ti-precursor was used (Ti-MgO/O).

XRD patterns for Ti-MgO samples show that both samples consist of a mixture of periclase (MgO) and geikielite ($MgTiO_3$), but the appearance of additional mixed phases

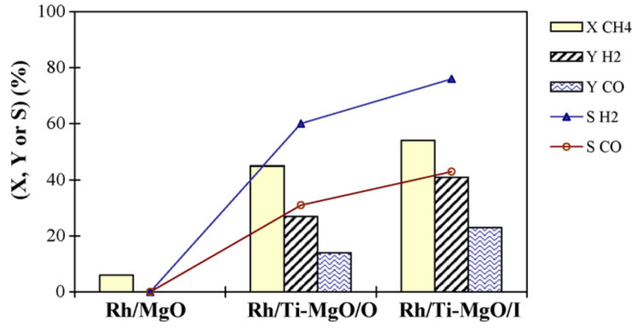

Fig. 5. Activity in POM reaction obtained over Rh-supported catalysts at 550 °C.

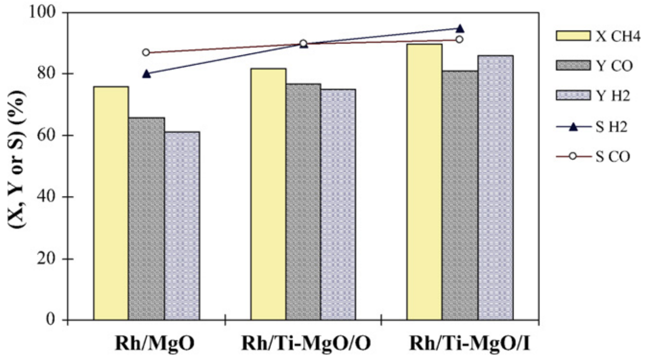

Fig. 6. Activity in POM reaction obtained over Rh-supported catalysts at 700 °C.

depends on the Ti-precursor. Indeed, qandilite (Mg_2TiO_4) or karooite ($MgTi_2O_5$) is observed for Ti-MgO/I and Ti-MgO/O, respectively. The large width of the peaks corresponding to the Mg-Ti-O phases can be accounted for the poor crystallinity or small size of the Ti-Mg mixed oxide particles and, on the other hand, for the possibility that Ti-Mg mixed oxide composition can vary slightly from particle to particle. No TiO_2 peaks are found, suggesting that either all titanium is found in the mixed phase Mg-Ti-O or TiO_2 crystallites are too small (<5 nm) for being resolved in XRD. These results differ from those reported by Tanabe et al. [12] for the same system, who only detected periclase, anatase and an amorphous phase. Their synthesis method, however, produces inhomogeneous samples. MgO-TiO_2 samples with different MgO:TiO_2 weight ratios were more recently prepared by the sol–gel method in [13]. In these MgO-TiO_2 samples, additional to periclase and anatase, three intermediate compounds were detected: karooite, geikielite and qandilite in concentrations that depended on MgO to TiO_2 weight ratio. It is clear from the above discussion that the structural properties of Ti-MgO systems strongly depend on the synthesis procedure. In addition, our results indicate that the precursor of Ti used for the synthesis of Ti-MgO systems, influence the solid state properties of the resulting samples. XPS data show that the inorganic precursor favours the deposition of Ti at the external surface of MgO (Table 1), suggesting again that the nature of the Ti-precursor affects on the properties of the resulting samples.

4.2. *Effect of the Ti-precursor on the solid state properties of Rh-supported catalysts*

It is well known that there are weak interactions between Rh and SiO_2. Literature shows that rhodium is reduced on this support at about 140 °C [1]. In contrast the peak at much higher temperature range (380–405 °C) in the TPR profile of our catalysts (Fig. 1) would imply that there are much stronger interactions between Rh and MgO-based supports.

The formation of $MgRh_2O_4$ was reported previously [14]. XRD patterns for Rh/MgO show the absence of $MgRh_2O_4$. XRD patterns for Rh(10)/MgO (10 wt.% of Rh), also calcined at 700 °C for 4 h, do not show the features of such a phase either. Thus, one can conclude that, in the conditions of the present study, no formation of this phase occurred. Therefore, the higher reduction temperatures of Rh on the catalysts are likely due to strong interactions between Rh and supports, which do not lead to a chemical compound. As mentioned earlier, the surface concentration of all the elements is not affected by the reaction atmosphere. Particularly, the constancy of the surface Rh concentration would indicate that the Rh dispersion remains constant after POM reaction, evidencing once more, that Rh interacts strongly with supports.

The reduction of rhodium on the different catalysts varies in the order: Ti-MgO/I > Ti-MgO/O > MgO and its reduction temperature is slightly higher for the Ti-containing catalysts. This suggests that interaction of Rh with Ti-containing supports is even stronger than in the case of the bare MgO support. Nevertheless, it is necessary to point out that such differences are tiny and must be carefully interpreted. XPS data revealed that there is a larger amount of metallic Rh on the Ti-containing catalysts. This phenomenon has been reported in a previous work [3] for Rh/Ti-SiO_2 catalysts. It was also demonstrated that the extent of Rh reduction enhances with the titania loading. In this case, differences in the Rh dispersion as well as in the Rh particles size for Ti-containing catalysts are believed to be responsible for the observed phenomena. Since in the present study, the characterization techniques do not reflect such changes, it can be only argued that the reduction of Rh on MgO can be promoted by adding titanium on it.

TPR results showed that reduction of Rh on Ti-MgO/I occurs at somewhat higher temperatures than on Ti-MgO/O, although differences are small. TPR profile of Rh/Ti-MgO/I differs from that of Rh/Ti-MgO/O (Fig. 1), which seems to indicate that reduction of Rh is up to a point affected by the Ti-precursor. It is well known that the ease of the reduction of Rh particles is related to their size: the smaller the particles, the easier the reduction. The size of Rh particles estimated by XPS indicates that both catalysts have particles comparable in size, which cannot explain differences in Rh reducibility. XPS also shows that the surface of the inorganic catalyst is considerably richer in Ti compared to the organic one (Table 1), and in this catalyst a larger amount of reduced Rh is found (XPS). This suggests again that the reducibility of Rh on Ti-MgO supports depends on the Ti-source, which is in line with the above observations. However, at this point, we have no additional evidences to support this observation.

For reduced catalysts, the BE of the $Rh3d_{5/2}$ peak is 306.5 eV, which is notably lower than the value for metallic Rh (307.0–307.3 eV). No similar shifts are seen in the peaks of the other components. This phenomenon has been reported in previous works [11], in that case authors proposed differential charging effects as one of the possible explanations for the unusually low Rh3d binding energy. In order to study this hypothesis, additional XPS measurements with an increased balance plate voltage (−4.8 V) were performed. As for the previous measurements, Rh3d peak was well shifted without presenting any deformation in the shape. On the basis of these results, the presence of any differential charging effect affecting the shape of the Rh3d peaks is excluded, but at this point we have no explanation for this extremely low value of the rhodium binding energy.

4.3. *Correlation between the solid state properties and the catalytic performance of Rh-supported catalysts*

The physico-chemical description of the catalysts given previously is consistent with the catalytic behaviour of these rhodium-containing formulations. It is observed that the higher the amount of reduced Rh (Rh/Ti-MgO/I), the higher the catalytic activity.

It is commonly accepted that metallic Rh is the active site for the partial oxidation of methane. As shown in Fig. 5 at low temperature Ti-containing catalysts are considerably more active than Rh/MgO. XPS results for the reduced catalysts revealed that rhodium is reduced in a larger extent on Ti-containing catalysts. Therefore, it can be assumed that on these catalysts, there are also a larger number of active sites for POM, which would explain the better performance of Ti-containing catalysts compared to the bare MgO. Catalytic results also show that the performance of Ti-containing catalysts slightly depends on the Ti-precursor, namely it is favoured when the inorganic Ti-precursor is used. This is particularly noticeable at low temperature (550 °C, Fig. 5). The properties of both Rh/Ti-MgO/I and Rh/Ti-MgO/O catalysts are not very different and the main difference between them is provided by XPS. Indeed, XPS for Rh/Ti-MgO/I after test at 550 °C (at this temperature differences in catalytic performance between both catalysts are remarkable) showed that there is a greatly larger amount of reduced Rh in this catalyst (Table 3). However, at higher temperatures (700 °C) Rh reduction is favoured and both catalysts have a similar amount of reduced Rh (and thus, a similar number of active sites for POM). This explains why at 700 °C, the catalytic performances of both catalysts are considerably smaller than at 550 °C. On the other hand, Ti is preferentially deposited at the external surface of MgO in Ti-MgO/I sample (XPS), which in turn have a larger amount of reduced Rh. These observations strongly suggest that metallic Rh is more easily generated on a Ti-rich surface. Since the rate or reaction is directly related to the state of Rh particles, the relative ease of generation of metallic Rh for the inorganic catalyst (Ti-rich surface) implies that it might be more active in POM in comparison with the organic one, which agrees with the catalytic results.

5. Conclusions

This paper shows that the performance of Rh-supported catalysts in the POM reaction can be improved by using Ti-MgO as supports. The catalytic behaviour of Rh-supported catalysts depends on the Ti-precursor. The inorganic Ti-precursor ($TiCl_4$) provides a Ti-rich surface, which seems to ease the generation of metallic rhodium resulting in an improvement of the performance of this catalyst.

Acknowledgements

The authors thank M.J. Genet for his fruitful advices about XPS technique. The authors gratefully acknowledge the ‘‘Direction Générale des Technologies, de la Recherche et de l’Energie (DGTRE)’’ of the ‘‘Région Wallonne’’ (Belgium) and the ‘‘Fonds National de la Recherche Scientifique (FNRS)’’ of Belgium, for their financial support. The involvement of the laboratory CATA in the Coordinated Action ‘‘CONCORDE’’, in the Network of Excellence ‘‘FAME’’ of the EU 6th FP, in the IUAP network ‘‘Supramolecularity’’ sustained by the ‘‘Service public fédéral de programmation politique scientifique’’ (Belgium), is acknowledged.

References

[1] H.Y. Wang, E. Ruckenstein, J. Catal. 186 (1999) 181.
[2] E. Ruckenstein, H.Y. Wang, J. Catal. 187 (1999) 151.
[3] C. Mateos-Pedrero, C. Cellier, P. Ruiz, Catal. Today 117 (2006) 362.
[4] H.-W. Jen, G.W. Graham, W. Chun, R.W. McCabe, J.-P. Cuif, S.E. Deutsch, O. Touret, Catal. Today 50 (1999) 309.
[5] K.F.W. Sing, D.H. Everet, R.A.W. Haul, L. Moscou, R.A. Pierotti, J. Rouquerol, T. Siemieniewska, Pure Appl. Chem. 57 (1985) 603.
[6] S. Sugiyama, T. Ookubo, K. Shimodan, H. Hayashi, J.B. Muffat, Bull. Chem. Soc. Jpn. 67 (1994) 3339.
[7] J.P. Nogier, A.M. De Kersabiec, J. Fraissard, Appl. Catal. A: Gen. 185 (1999) 109.
[8] J. Huuhtanen, M. Sanati, A. Andersson, T.A. Lars, Appl. Catal. A: Gen. 97 (1993) 197.
[9] Z. Weng-Siegh, R. Gronsky, A.T. Bell, J. Catal. 170 (1997) 62.
[10] J.L.G. Fierro, J.M. Palacios, F. Tomas, Surf. Interface Anal. 13 (1988) 25.
[11] R. Polvinen, M. Vippola, M. Valden, T. Lepistö, A. Suopanki, M. Härkönen, Surf. Interface Anal. 36 (2004) 741.
[12] K. Tanabe, H. Hattori, T. Yumiyoshi, K. Tanaru, T. Kondo, J. Catal. 53 (1978) 1.
[13] T. López, J. Hernández, R. Gómez, Langmuir 15 (1999) 5689.
[14] E. Ruckenstein, H.Y. Wang, Appl. Catal. A: Gen. 198 (2000) 33.